




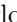
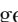







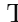






K. Trabelsi , I. Tsaklidis , M. Uchida , I. Ueda , Y. Uematsu , T. Uglov , K. Unger , Y. Unno , K. Uno ,
 S. Uno , P. Urquijo , Y. Ushiroda , S. E. Vahsen , R. van Tonder , G. S. Varner , K. E. Varvell ,
 M. Veronesi , V. S. Vismaya , L. Vitale , V. Vobbiliseti , R. Volpe , B. Wach , E. Waheed , M. Wakai ,
 S. Wallner , E. Wang , M.-Z. Wang , Z. Wang , A. Warburton , M. Watanabe , S. Watanuki , M. Welsch ,
 C. Wessel , X. P. Xu , B. D. Yabsley , S. Yamada , W. Yan , S. B. Yang , J. H. Yin , K. Yoshihara ,
 C. Z. Yuan , L. Zani , Y. Zhang , V. Zhilich , J. S. Zhou , Q. D. Zhou , V. I. Zhukova , and R. Žlebčák

(The Belle II Collaboration)

We present the first comprehensive tests of the universality of the light leptons in the angular distributions of semileptonic B^0 -meson decays to charged spin-1 charmed mesons. We measure five angular-asymmetry observables as functions of the decay recoil that are sensitive to lepton-universality-violating contributions. We use events where one neutral B is fully reconstructed in $\Upsilon(4S) \rightarrow B\bar{B}$ decays in data corresponding to 189 fb^{-1} integrated luminosity from electron-positron collisions collected with the Belle II detector. We find no significant deviation from the standard model expectations.

In the standard model, all leptons share the same electroweak coupling, a symmetry known as lepton universality (LU). Semileptonic B -meson decays involving the quark transition $b \rightarrow c\ell\nu$ provide excellent sensitivity to potential new interactions that would violate this symmetry. Evidence for lepton-universality violation (LUV) in the ratio of semileptonic decay rates to τ leptons relative to the light-leptons ℓ , denoting electrons and muons, has been reported in the combination of results from the BaBar, Belle, and LHCb Collaborations [1–8]. Recently, evidence of LUV between the light leptons at the four-standard-deviation level has been reported based on differences in their angular distributions in semileptonic B decays to D^* mesons [9]. However, that analysis relied on a reinterpretation of Belle results [10] that contained only one-dimensional projections of the multidimensional angular distributions that are needed to fully characterize such decays. We present the first light-lepton LU test using a complete set of angular-asymmetry observables chosen to suppress most theoretical and experimental uncertainties, thus optimizing sensitivity to LUV [11]. This test is complementary to the branching-fractions-based LUV test in Ref. [12].

The semileptonic decay $B^0 \rightarrow D^{*-}\ell\nu$ is mediated in the standard model via W -boson exchange (charge conjugation is implied throughout). Due to the spin of the D^{*-} , which is reconstructed from its decay to a \bar{D}^0 and a charged pion, the properties of the coupling and the spin of the virtual W are encoded in angular distributions of the final-state particles. These can be fully characterized in terms of a recoil parameter and three helicity angles. The recoil parameter is defined as

$$w \equiv \frac{m_{B^0}^2 + m_{D^{*-}}^2 - q^2}{2m_B m_{D^*}}, \quad (1)$$

where m_{B^0} and m_{D^*} are the known B^0 and D^{*-} masses and q is the four-vector of the momentum transferred to the dilepton system (natural units are used throughout). The helicity angles are defined as follows: θ_ℓ is the angle

between the direction of the charged lepton in the virtual W frame and the W in the B^0 frame, θ_V is the angle between the \bar{D}^0 direction in the D^{*-} frame and the D^{*-} in the B^0 frame, and χ is the angle between the decay planes formed by the virtual W and the D^{*-} in the B^0 frame. Of these angles, only θ_ℓ is correlated to lab-frame quantities.

The four-dimensional standard-model differential rate can be represented in terms of eight helicity amplitudes and as a function of w , $\cos\theta_\ell$, $\cos\theta_V$, and χ [13, 14]. It is possible to construct one- or two-dimensional integrals of these differential rates to isolate angular asymmetries that are sensitive to LUV, called A_{FB} , S_3 , S_5 , S_7 , and S_9 [11]. The forward-backward asymmetry A_{FB} measures the tendency for the charged lepton to travel in the same direction as the virtual W . The S_3 and S_9 asymmetries are sensitive to the alignment of the lepton and D^* momenta, while S_5 and S_7 measure coupled alignments in the orientation of the D with respect to the D^* . We redefine these asymmetries in terms of one-dimensional integrals

$$\mathcal{A}_x(w) \equiv \left(\frac{d\Gamma}{dw}\right)^{-1} \left[\int_0^1 - \int_{-1}^0 \right] dx \frac{d^2\Gamma}{dw dx}, \quad (2)$$

with $x = \cos\theta_\ell$ for A_{FB} , $\cos 2\chi$ for S_3 , $\cos\chi \cos\theta_V$ for S_5 , $\sin\chi \cos\theta_V$ for S_7 , and $\sin 2\chi$ for S_9 , as illustrated in the supplemental material [15]. The determination of each of the five asymmetries then reduces to measuring the signal yields N_x^- with $x \in [-1, 0)$ and N_x^+ with $x \in [0, 1]$ after accounting for experimental effects such as resolution and detector acceptance. The asymmetries are then calculated as

$$\mathcal{A}_x(w) = \frac{N_x^+(w) - N_x^-(w)}{N_x^+(w) + N_x^-(w)}. \quad (3)$$

The differences between the angular asymmetries of electrons and muons,

$$\Delta\mathcal{A}_x(w) \equiv \mathcal{A}_x^\mu(w) - \mathcal{A}_x^e(w), \quad (4)$$

are sensitive to interactions that violate LU. Most experimental uncertainties cancel in the asymmetries \mathcal{A}_x , and standard-model contributions largely cancel in the asymmetry differences $\Delta\mathcal{A}_x$, only arising from the differences in lepton masses. Therefore, the compatibility between measurements of the asymmetry differences $\Delta\mathcal{A}_x$ and their standard-model expectations is a powerful test of LU. To optimize sensitivity to extensions of the standard model [11], we measure these variables integrated over three w ranges: the full phase-space ($w_{\text{incl.}}$), the low w region (w_{low}) from 1 up to 1.275, and the high w region (w_{high}) from 1.275 to the kinematic endpoint at 1.503.

For each asymmetry \mathcal{A}_x and w range, we separate signal candidates into angular categories $+$ and $-$ based on the measured value of x . We determine the numbers of signal events N_x^\pm with fits to distributions of M_{miss}^2 , the squared difference between the sum of the four-momenta of the colliding particles and the sum of the four-momenta of the reconstructed particles. The M_{miss}^2 distribution for correctly reconstructed signal events peaks near zero, while the distribution for backgrounds, which come mostly from $B \rightarrow D^{**}\ell\nu$ decays, does not peak. We correct these event numbers for detector efficiency, acceptance, and resolution effects determined from simulation in order to calculate unbiased asymmetries.

Of the five asymmetries, only A_{FB} and S_3 have been measured, but not differentially in w [9, 16, 17]. In the standard model or any extension thereof, S_9 is always zero [9]. Similarly, S_7 is always zero in the standard model and has reduced sensitivity to its extensions [11]. In contrast, A_{FB} , S_3 , and S_5 are highly sensitive to LUV via their asymmetry differences, which should show highly correlated deviations from the SM expectations in the case of new interactions. Therefore, correlated LUV signatures between the asymmetry differences can help to probe the nature of any new interactions. Therefore, the simultaneous determination of all asymmetries in different w ranges provides a powerful test of LU and probes the nature of non-standard-model interactions.

We measure the asymmetries and their differences using a dataset corresponding to 189 fb^{-1} of electron-positron collisions at 10.58 GeV center-of-mass energy collected by the Belle II experiment between 2019 and 2021. We use the Belle II detector [18] to reconstruct $\Upsilon(4S) \rightarrow B^0\bar{B}^0$ decays. The detector consists of several nested subsystems in a cylindrical barrel, closed on either end with endcaps, arranged around the interaction region and nearly coaxial with the beams. The innermost subsystem is the vertex detector, composed of two layers of silicon pixels and four outer layers of silicon-strip detectors. During data collection for this analysis the outermost pixel layer only covered 15% of the azimuth. Charged-particle trajectories (tracks) are reconstructed by a small-cell drift chamber (CDC) filled with a He 50% and C_2H_6 50% gas mixture, which also provides a measurement of ionization energy-loss for parti-

cle identification. A Cherenkov-light imaging and time-of-propagation detector (TOP) provides charged pion and kaon identification information in the barrel region. This information is provided in the forward endcap by a proximity-focusing, ring-imaging Cherenkov detector with an aerogel radiator. An electromagnetic calorimeter (ECL) consisting of CsI(Tl) crystals provides neutral-particle and electron identification information in the barrel and both endcaps. All of the above subsystems are immersed in a uniform 1.5 T magnetic field that is nearly aligned with the electron beam and is generated by a superconducting solenoid situated outside the calorimeter. The outermost subsystem, the K_L^0 and muon identification detector, consists of scintillator strips in the endcaps and the inner part of the barrel, and resistive-plate chambers in the outer barrel, interleaved with iron plates that serve as a magnetic flux-return yoke.

We use Monte Carlo (MC) simulation to model the signal and backgrounds and to calculate reconstruction efficiencies. We use the software libraries `EvtGen` [19], `PYTHIA` [20], and `KKMC` [21] to model particle production and decay, `PHOTOS` [22] for photon radiation, and `GEANT4` [23] for detector response. We overlay simulated beam-induced backgrounds on the simulated events [24]. We simulate 900 fb^{-1} of $B^0 \rightarrow D^{*-}\ell\nu$ decays with the form factors of Refs. [25–27] and values determined by the measurements of Refs. [10]. We use the Belle II analysis software, `basf2` [28, 29], to reconstruct simulated and experimental data identically.

In each event, we use the full event interpretation (FEI) algorithm [30] to fully reconstruct one neutral B^0 , called the tag B^0 . The FEI reconstructs tag B^0 candidates in explicit hadronic decay cascades with no missing particles. Each tag B^0 candidate then consists of a collection of detected tracks and neutral energy depositions (clusters) and a hypothesis for the full B^0 decay cascade that produced them. We use three variables to select correctly reconstructed tags. The beam-constrained mass M_{bc} is calculated from the center-of-mass collision energy \sqrt{s} and tag- B momentum \vec{p}_B ,

$$M_{\text{bc}} = \sqrt{(\sqrt{s}/2)^2 - |\vec{p}_B|^2}. \quad (5)$$

The energy difference $\Delta E = E_B - \sqrt{s}/2$ is the difference between the center-of-mass collision energy and tag- B energy E_B . Finally, a tag-reconstruction confidence score, \mathcal{P}_{FEI} , valued between zero and one, quantifies the agreement between the kinematic properties of the detected particles and the hypothesized decay cascade.

Correctly and completely reconstructed B^0 candidates have M_{bc} near the B^0 mass, ΔE near zero, and \mathcal{P}_{FEI} near 1. We require that tag B^0 candidates satisfy $M_{\text{bc}} > 5.27 \text{ GeV}$, $\Delta E \in [-0.15, 0.1] \text{ GeV}$, and $\mathcal{P}_{\text{FEI}} > 0.001$. If multiple tag B^0 candidates in an event pass these selections, we keep only the one with the highest value of \mathcal{P}_{FEI} .

In events with an identified tag B^0 candidate, we reconstruct $B^0 \rightarrow D^{*-}(\rightarrow \bar{D}^0\pi^-)\ell\nu$ candidates with \bar{D}^0 decaying to $K^+\pi^-$, $K^+\pi^-\pi^+\pi^-$, $K^+\pi^-\pi^0$, $K^+\pi^-\pi^+\pi^-\pi^0$, $K_s^0\pi^+\pi^-$, $K_s^0\pi^+\pi^-\pi^0$, $K_s^0\pi^0$, or K^+K^- final states. We require that all tracks originate from the vicinity of the interaction point. We require that each lepton candidate have a lab-frame momentum above 0.4 GeV, and a polar angle within the range $[0.22, 2.71]$ rad for electrons and $[0.4, 2.6]$ rad for muons, to ensure that suitable particle-identification information is available. Leptons are identified using the ratio of their likelihood to the sum of likelihoods for all charged-particle types. These likelihoods combine particle-identification information from the CDC, ECL, and, for muons, the TOP. We retain lepton candidates with a likelihood ratio above 0.9, resulting in electron and muon identification efficiencies of 86% and 89%, respectively, and hadron misidentification rates of less than 1% and 3%, respectively. We determine lepton-identification efficiencies and their uncertainties from auxiliary measurements in discrete intervals of lab-frame momentum, polar angle, and charge, using $J/\psi \rightarrow \ell^+\ell^-$, $e^+e^- \rightarrow \ell^+\ell^-(\gamma)$, and $e^+e^- \rightarrow (e^+e^-)\ell^+\ell^-$ events.

We reconstruct π^0 candidates via decays to two photons. We identify photon candidates from ECL clusters unassociated with any matched tracks and with timing selections designed to minimize contamination from beam-induced backgrounds. We require that each π^0 candidate have an invariant mass in the range $[0.120, 0.145]$ GeV, approximately four times the diphoton mass resolution. The π^0 reconstruction and selection efficiency is approximately 0.3.

We reconstruct K_s^0 candidates via decays to two charged particles that are assigned the pion mass. We require that each K_s^0 candidate has an invariant mass in the range $[0.3, 0.7]$ GeV and that it can be fit to a common vertex that is displaced from the interaction point by at least one unit of the uncertainty of the vertex fit. We also require that the angle between the momentum of the K_s^0 candidate and the displacement of the vertex from the interaction point be less than 0.64 rad.

We require that the mass of each \bar{D}^0 candidate is in the range $[1.85, 1.88]$ GeV, corresponding to approximately four times the peak resolution and centered on the known mass. We reconstruct D^{*-} candidates by combining \bar{D}^0 candidates with each of the remaining tracks, which we label π_{slow} , and require that the mass difference between the \bar{D}^0 and D^{*-} candidates is in the range $[0.143, 0.148]$ GeV, approximately four times its resolution.

We combine D^{*-} and lepton candidates to form signal B^0 candidates and use the `TreeFit` [31] algorithm to reject candidates that cannot be fit to consistent vertices. We then combine the signal and tag B^0 candidates and require that no additional tracks remain in the event and that the difference between the reconstructed energy and

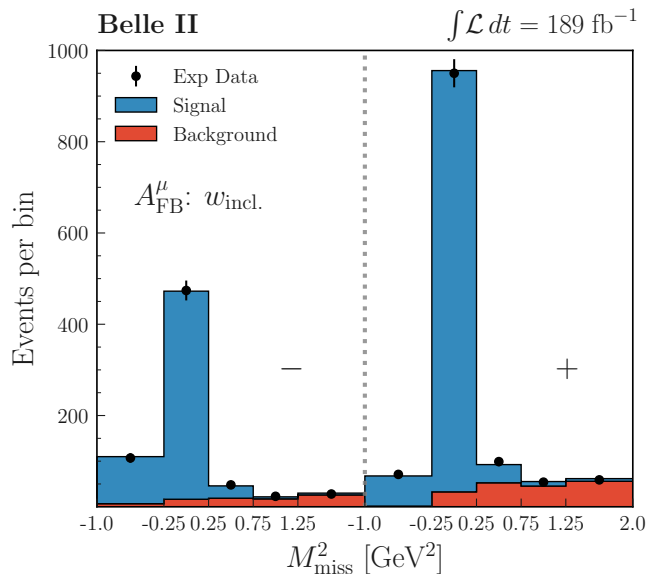


Figure 1: Muon-mode M_{miss}^2 distributions and fit results for $\cos\theta_\ell$ in the ranges $[-1, 0]$ (left) and $[0, 1]$ (right), corresponding to the $-$ and $+$ categories of A_{FB}^μ , in the full w range ($w_{\text{incl.}}$).

the collision energy is greater than 0.3 GeV, in order to reject hadronic decay backgrounds. If more than one candidate passes these requirements, we select only the one closest to expectation in the well-modeled quantity $|M(D^*) - M(D)|$.

We obtain the signal yield for each combination of lepton flavor, w interval, and angular category ($+$ or $-$ as defined for a particular asymmetry \mathcal{A}_x) using a binned maximum-likelihood fit to the distribution of M_{miss}^2 . The signal yield $N_x^\pm(w)$ and the background yield are unconstrained in the fit, allowing for an effective background-subtraction that removes dependence on the angular asymmetry of the backgrounds. We determine the shapes of the signal and background with simulation and choose a coarse binning to minimize dependence on resolution modeling. In Fig. 1 we show the two such independent fits that determine N_x^+ and N_x^- for $x = \cos\theta_\ell$ in the muon mode and in the $w_{\text{incl.}}$ bin. Together, these yields determine $A_{\text{FB}}^\mu(w_{\text{incl.}})$. We find 1617 (1639) signal events in the electron (muon) mode overall, with a variation of less than one event between variables. Of these, 803 (853) are in the w_{low} range.

We correct the fitted yields $N_x^\pm(w)$ for selection and detector acceptance losses using efficiency estimates from simulation. The efficiency ratios between the $+$ and $-$ categories are typically near 1.0 but range up to nearly 1.4 for A_{FB}^μ , largely due to the reduced momentum of leptons in the $-$ category, which are emitted opposite to the direction of the boost of the B mesons, relative to the $+$ leptons, which are emitted in the direction of the boost. This lower momentum results in lower reconstruction and

Table I: Summary of the results and comparison with expectations. The measurement uncertainties are statistical and systematic, respectively.

Obs.	w bin	$\Delta\mathcal{A}_x$	SM expectation
ΔA_{FB}	w_{low}	$0.099 \pm 0.056 \pm 0.020$	-0.00104
	w_{high}	$-0.168 \pm 0.068 \pm 0.024$	-0.01133
	$w_{\text{incl.}}$	$-0.024 \pm 0.043 \pm 0.016$	-0.00566
ΔS_3	w_{low}	$-0.026 \pm 0.068 \pm 0.024$	0.00028
	w_{high}	$-0.101 \pm 0.069 \pm 0.025$	0.00023
	$w_{\text{incl.}}$	$-0.062 \pm 0.047 \pm 0.017$	0.00018
ΔS_5	w_{low}	$-0.019 \pm 0.068 \pm 0.024$	0.00027
	w_{high}	$-0.055 \pm 0.065 \pm 0.023$	0.00107
	$w_{\text{incl.}}$	$-0.035 \pm 0.046 \pm 0.016$	0.00049
ΔS_7	w_{low}	$0.028 \pm 0.067 \pm 0.024$	0
	w_{high}	$-0.066 \pm 0.065 \pm 0.022$	0
	$w_{\text{incl.}}$	$-0.026 \pm 0.046 \pm 0.016$	0
ΔS_9	w_{low}	$0.032 \pm 0.067 \pm 0.024$	0
	w_{high}	$0.020 \pm 0.068 \pm 0.024$	0
	$w_{\text{incl.}}$	$0.020 \pm 0.047 \pm 0.017$	0

identification efficiencies. We further correct for migration of candidates between the + and - categories and different w bins by inverting a detector-response matrix. This matrix is constructed from the conditional probabilities that events generated in a particular kinematic bin are reconstructed in each kinematic bin. For every variable and bin, the probability of reconstruction into the correct bin is above 0.86.

The largest systematic uncertainty affecting the measurement is from the size of the simulated samples, which limits the precision of the bin-migration and efficiency corrections. We determine this uncertainty from the standard deviation of the results obtained by repeatedly resampling the simulated data with replacement and re-fitting. This uncertainty is approximately one-fourth to one-half of the statistical uncertainty, ranging in 0.010–0.025. We determine the uncertainties from other systematic effects by varying their contribution within their known uncertainties or bounds [32] or from independent control data. Lepton-identification uncertainties mostly cancel in the asymmetries \mathcal{A} and are at most 0.004. The uncertainty on the reconstruction efficiency of π_{slow} also largely cancels and is negligible. Uncertainties from modeling of the background processes, such as $B \rightarrow D^{**} \ell \bar{\nu}_\ell$, are negligible due to fitting the backgrounds independently in + and - categories. The supplemental material contains a full list of all of the systematic uncertainties [15].

Figure 2 shows our measurements of the asymmetries and the LUV-sensitive differences and Table I shows the numerical values. The numerical values and full covariance matrices of the measured observables will be made available on HEPData [33]. These measurements are the first comprehensive tests of lepton universality in the angular distributions of semileptonic B decays. We

compare our measurements to predictions from Ref. [34] and measurements from Refs. [9, 16, 17]. The results in Ref. [9] are obtained in a slightly reduced w range, [1, 1.5], which makes them not strictly comparable to the other results. However, the standard-model expectations in these two w ranges differ only in the fourth decimal place. The results from Refs. [9, 17] derive from analyses without explicit reconstruction of the tag B , resulting in lower statistical uncertainties relative to these results.

To test agreement with the standard-model expectation [34], we perform three different χ^2 tests, accounting for the statistical and systematic covariances between all of the variables. Tests of the asymmetries \mathcal{A} in the full w range ($w_{\text{incl.}}$) yield $\chi^2/N_{\text{dof}} = 14.6/10$ ($p = 0.15$) and in w subranges ($w_{\text{low}}, w_{\text{high}}$) yield 26.7/20 ($p = 0.14$). Tests of the LUV-sensitive asymmetry differences ΔA_{FB} , ΔS_3 , and ΔS_5 in the $w_{\text{incl.}}$ range yield $\chi^2/N_{\text{dof}} = 2.0/3$ ($p = 0.57$) and in w subranges yield 10.2/6 ($p = 0.13$). Tests of the insensitive quantities ΔS_7 and ΔS_9 in the $w_{\text{incl.}}$ range yield $\chi^2/N_{\text{dof}} = 0.6/2$ ($p = 0.76$) and in w subranges yield 1.5/4 ($p = 0.83$). Our results agree well with the standard-model expectations and provide no evidence for LUV.

This work, based on data collected using the Belle II detector, which was built and commissioned prior to March 2019, was supported by Science Committee of the Republic of Armenia Grant No. 20TTCG-1C010; Australian Research Council and research Grants No. DE220100462, No. DP180102629, No. DP170102389, No. DP170102204, No. DP150103061, No. FT130100303, No. FT130100018, and No. FT120100745; Austrian Federal Ministry of Education, Science and Research, Austrian Science Fund No. P 31361-N36 and No. J4625-N, and Horizon 2020 ERC Starting Grant No. 947006 “InterLeptons”; Natural Sciences and Engineering Research Council of Canada, Compute Canada and CANARIE; Chinese Academy of Sciences and research Grant No. QYZDJ-SSW-SLH011, National Natural Science Foundation of China and research Grants No. 11521505, No. 11575017, No. 11675166, No. 11761141009, No. 11705209, and No. 11975076, LiaoNing Revitalization Talents Program under Contract No. XLYC1807135, Shanghai Pujiang Program under Grant No. 18PJ1401000, Shandong Provincial Natural Science Foundation Project ZR2022JQ02, and the CAS Center for Excellence in Particle Physics (CCEPP); the Ministry of Education, Youth, and Sports of the Czech Republic under Contract No. LTT17020 and Charles University Grant No. SVV 260448 and the Czech Science Foundation Grant No. 22-18469S; European Research Council, Seventh Framework PEF-GA-2013-622527, Horizon 2020 ERC-Advanced Grants No. 267104 and No. 884719, Horizon 2020 ERC-Consolidator Grant No. 819127, Horizon 2020 Marie Skłodowska-Curie Grant Agreement No. 700525 “NIOBE” and No. 101026516, and Horizon 2020 Marie Skłodowska-Curie RISE project

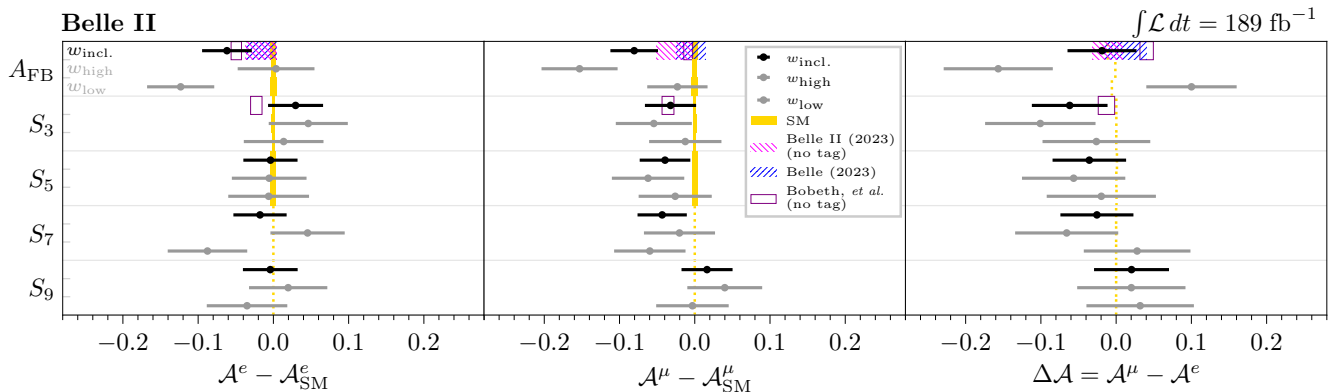


Figure 2: Observed asymmetries and their differences (points with error bars), one-standard-deviation bands from the Belle [16] and Belle II [17] measurements (hatched boxes), calculations from Ref. [9] based on a previous measurement from Belle [10] (empty boxes), and standard-model expectations (solid boxes). The standard-model expectation is drawn with a dashed line when its uncertainty is too small to display.

JENNIFER2 Grant Agreement No. 822070 (European grants); L'Institut National de Physique Nucléaire et de Physique des Particules (IN2P3) du CNRS (France); BMBF, DFG, HGF, MPG, and AvH Foundation (Germany); Department of Atomic Energy under Project Identification No. RTI 4002 and Department of Science and Technology (India); Israel Science Foundation Grant No. 2476/17, U.S.-Israel Binational Science Foundation Grant No. 2016113, and Israel Ministry of Science Grant No. 3-16543; Istituto Nazionale di Fisica Nucleare and the research grants BELLE2; Japan Society for the Promotion of Science, Grant-in-Aid for Scientific Research Grants No. 16H03968, No. 16H03993, No. 16H06492, No. 16K05323, No. 17H01133, No. 17H05405, No. 18K03621, No. 18H03710, No. 18H05226, No. 19H00682, No. 22H00144, No. 26220706, and No. 26400255, the National Institute of Informatics, and Science Information NETWORK 5 (SINET5), and the Ministry of Education, Culture, Sports, Science, and Technology (MEXT) of Japan; National Research Foundation (NRF) of Korea Grants No. 2016R1D1A1B-02012900, No. 2018R1A2B3003643, No. 2018R1A6A1A-06024970, No. 2018R1D1A1B07047294, No. 2019R1-I1A3A01058933, No. 2022R1A2C1003993, and No. RS-2022-00197659, Radiation Science Research Institute, Foreign Large-size Research Facility Application Supporting project, the Global Science Experimental Data Hub Center of the Korea Institute of Science and Technology Information and KREONET/GLORIAD; Universiti Malaya RU grant, Akademi Sains Malaysia, and Ministry of Education Malaysia; Frontiers of Science Program Contracts No. FOINS-296, No. CB-221329, No. CB-236394, No. CB-254409, and No. CB-180023, and No. SEP-CINVESTAV research Grant No. 237 (Mexico); the Polish Ministry of Science and Higher Education and the National Science Center; the Ministry of

Science and Higher Education of the Russian Federation, Agreement No. 14.W03.31.0026, and the HSE University Basic Research Program, Moscow; University of Tabuk research Grants No. S-0256-1438 and No. S-0280-1439 (Saudi Arabia); Slovenian Research Agency and research Grants No. J1-9124 and No. P1-0135; Agencia Estatal de Investigación, Spain Grant No. RYC2020-029875-I and Generalitat Valenciana, Spain Grant No. CIDE-GENT/2018/020 Ministry of Science and Technology and research Grants No. MOST106-2112-M-002-005-MY3 and No. MOST107-2119-M-002-035-MY3, and the Ministry of Education (Taiwan); Thailand Center of Excellence in Physics; TUBITAK ULAKBIM (Turkey); National Research Foundation of Ukraine, project No. 2020.02/0257, and Ministry of Education and Science of Ukraine; the U.S. National Science Foundation and research Grants No. PHY-1913789 and No. PHY-2111604, and the U.S. Department of Energy and research Awards No. DE-AC06-76RLO1830, No. DE-SC0007983, No. DE-SC0009824, No. DE-SC0009973, No. DE-SC0010007, No. DE-SC0010073, No. DE-SC0010118, No. DE-SC0010504, No. DE-SC0011784, No. DE-SC0012704, No. DE-SC0019230, No. DE-SC0021274, No. DE-SC0022350; and the Vietnam Academy of Science and Technology (VAST) under Grant No. DL0000.05/21-23.

These acknowledgements are not to be interpreted as an endorsement of any statement made by any of our institutes, funding agencies, governments, or their representatives.

We thank the SuperKEKB team for delivering high-luminosity collisions; the KEK cryogenics group for the efficient operation of the detector solenoid magnet; the KEK computer group and the NII for on-site computing support and SINET6 network support; and the raw-data centers at BNL, DESY, GridKa, IN2P3, INFN, and the

University of Victoria for offsite computing support.

-
- [1] J. P. Lees *et al.* (BaBar Collaboration), Evidence for an excess of $\bar{B} \rightarrow D^{(*)} \tau^- \bar{\nu}_\tau$ decays, *Phys. Rev. Lett.* **109**, 101802 (2012).
- [2] J. P. Lees *et al.* (BaBar Collaboration), Measurement of an excess of $\bar{B} \rightarrow D^{(*)} \tau^- \bar{\nu}_\tau$ decays and implications for charged Higgs bosons, *Phys. Rev. D* **88**, 072012 (2013).
- [3] M. Huschle *et al.* (Belle Collaboration), Measurement of the branching ratio of $\bar{B} \rightarrow D^{(*)} \tau^- \bar{\nu}_\tau$ relative to $\bar{B} \rightarrow D^{(*)} \ell^- \bar{\nu}_\ell$ decays with hadronic tagging at Belle, *Phys. Rev. D* **92**, 072014 (2015).
- [4] G. Caria *et al.* (Belle Collaboration), Measurement of $R(D)$ and $R(D^*)$ with a semileptonic t -tagging method, *Phys. Rev. Lett.* **124** (2020).
- [5] S. Hirose *et al.* (Belle Collaboration), Measurement of the τ lepton polarization and $R(D^*)$ in the decay $\bar{B} \rightarrow D^* \tau^- \bar{\nu}_\tau$, *Phys. Rev. Lett.* **118**, 211801 (2017).
- [6] R. Aaij *et al.* (LHCb Collaboration), Measurement of the ratio of branching fractions $\mathcal{B}(\bar{B}^0 \rightarrow D^{*+} \tau^- \bar{\nu}_\tau) / \mathcal{B}(\bar{B}^0 \rightarrow D^{*+} \mu^- \bar{\nu}_\mu)$, *Phys. Rev. Lett.* **115**, 111803 (2015), [Erratum: *Phys. Rev. Lett.* **115**, 159901 (2015)].
- [7] R. Aaij *et al.* (LHCb Collaboration), Measurement of the ratio of the $B^0 \rightarrow D^{*-} \tau^+ \nu_\tau$ and $B^0 \rightarrow D^{*-} \mu^+ \nu_\mu$ branching fractions using three-prong τ -lepton decays, *Phys. Rev. Lett.* **120**, 171802 (2018).
- [8] R. Aaij *et al.* (LHCb Collaboration), Test of lepton flavor universality by the measurement of the $B^0 \rightarrow D^{*-} \tau^+ \nu_\tau$ branching fraction using three-prong τ decays, *Phys. Rev. D* **97**, 072013 (2018).
- [9] C. Bobeth *et al.*, Lepton-flavour non-universality of $\bar{B} \rightarrow D^* \ell \bar{\nu}$ angular distributions in and beyond the Standard Model, *Eur. Phys. J. C* **81**, 984 (2021).
- [10] E. Waheed *et al.* (Belle Collaboration), Measurement of the CKM matrix element $|V_{cb}|$ from $B^0 \rightarrow D^{*-} \ell^+ \nu_\ell$ at Belle, *Phys. Rev. D* **100**, 052007 (2019), [Erratum: *Phys. Rev. D* **103**, 079901 (2021)].
- [11] B. Bhattacharya *et al.*, Implications for the ΔA_{FB} anomaly in $\bar{B}^0 \rightarrow D^{*+} \ell^- \bar{\nu}$ using a new Monte Carlo event generator, *Phys. Rev. D* **107**, 015011 (2023).
- [12] L. Aggarwal *et al.* (Belle II Collaboration), Test of Light-Lepton Universality in the Rates of Inclusive Semileptonic B -Meson Decays at Belle II, *Phys. Rev. Lett.* **131**, 051804 (2023).
- [13] J. G. Korner and G. A. Schuler, Exclusive semileptonic heavy meson decays including lepton mass effects, *Z. Phys. C* **46**, 93 (1990).
- [14] F. J. Gilman and R. L. Singleton, Analysis of semileptonic decays of mesons containing heavy quarks, *Phys. Rev. D* **41**, 142 (1990).
- [15] See Supplemental Material at <http://link.aps.org/supplemental/10.1103/PhysRevLett.131.181801> for additional information regarding construction of asymmetry integrals, statistical and systematic uncertainties, and covariance matrices.
- [16] M. T. Prim *et al.* (Belle Collaboration), Measurement of Differential Distributions of $B \rightarrow D^* \ell \bar{\nu}_\ell$ and Implications on $|V_{cb}|$ arXiv:2301.07529 (2023).
- [17] I. Adachi *et al.* (Belle II Collaboration), Determination of $|V_{cb}|$ using $\bar{B}^0 \rightarrow D^{*+} \ell^- \bar{\nu}_\ell$ decays with Belle II, Submitted to *Phys. Rev. D* (2023), arXiv:2310.01170 [hep-ex].
- [18] T. Abe (Belle II Collaboration), Belle II technical design report (2010), arXiv:1011.0352.
- [19] D. J. Lange, The EvtGen particle decay simulation package, *Nucl. Instrum. Meth. A* **462**, 152 (2001).
- [20] T. Sjöstrand *et al.*, An introduction to PYTHIA 8.2, *Comput. Phys. Commun.* **191**, 159 (2015).
- [21] S. Jadach *et al.*, The Precision Monte Carlo event generator KK for two fermion final states in e^+e^- collisions, *Comput. Phys. Commun.* **130**, 260 (2000).
- [22] E. Barberio, B. van Eijk, and Z. Was, PHOTOS: A Universal Monte Carlo for QED radiative corrections in decays, *Comput. Phys. Commun.* **66**, 115 (1991).
- [23] S. Agostinelli *et al.* (GEANT4 Collaboration), GEANT4—a simulation toolkit, *Nucl. Instrum. Meth. A* **506**, 250 (2003).
- [24] A. Natochii *et al.*, Beam background expectations for Belle II at SuperKEKB, (2022), arXiv:2203.05731.
- [25] C. G. Boyd, B. Grinstein, and R. F. Lebed, Constraints on form-factors for exclusive semileptonic heavy to light meson decays, *Phys. Rev. Lett.* **74**, 4603 (1995).
- [26] B. Grinstein and A. Kobach, Model-independent extraction of $|V_{cb}|$ from $\bar{B} \rightarrow D^* \ell \bar{\nu}$, *Phys. Lett. B* **771**, 359 (2017).
- [27] D. Bigi, P. Gambino, and S. Schacht, A fresh look at the determination of $|V_{cb}|$ from $B \rightarrow D^* \ell \nu$, *Phys. Lett. B* **769**, 441 (2017).
- [28] T. Kuhr *et al.* (Belle II Framework Software Group), The Belle II Core Software, *Comput. Softw. Big Sci.* **3**, 1 (2019).
- [29] The Belle II Collaboration, Belle II Analysis Software Framework (basf2) (2022).
- [30] T. Keck *et al.*, The Full Event Interpretation: An exclusive tagging algorithm for the Belle II experiment, *Comput. Softw. Big Sci.* **3**, 6 (2019).
- [31] W. Hulsbergen, The global covariance matrix of tracks fitted with a Kalman filter and an application in detector alignment, *Nucl. Instr. Meth. A* **600**, 471 (2009).
- [32] R. L. Workman *et al.* (Particle Data Group), Review of Particle Physics, *PTEP* **2022**, 083C01 (2022).
- [33] <https://www.hepdata.net/record/144759>.
- [34] F. U. Bernlochner *et al.*, Constrained second-order power corrections in HQET: $R(D^{(*)})$, $|V_{cb}|$, and new physics, *Phys. Rev. D* **106**, 096015 (2022).